JOURNAL OF MATERIALS SCIENCE 22 (1987) 2470–2476

The role of crazes in the crack growth of polyethylene

A. LUSTIGER*
Battelle-Columbus Division, 505 King Avenue, Columbus, Ohio, 43201-2693, USA
R. D. CORNELIUSSEN
Materials Engineering Department, Drexel University, Philadelphia, Pennsylvania 19104, USA

Brittle slow crack growth, or stress cracking, is a major concern in many applications of polyethylene materials. Using a constant tensile load test and removing specimens prior to complete failure, details of the crack tip region can be discerned in both butene and hexene copolymerized polyethylene. In both the presence and absence of an accelerating environment (Igepal CO-630), it was found that crazes formed at the crack tip, although secondary crazes were also evident in the specimens removed from the Igepal. Multiple crack arrest lines were clearly evident, suggesting a stick–slip mechanism under static load. The appearance of the craze zone at the crack tip can be explained through invoking an interlamellar failure model.

1. Introduction

The term "brittle failure" is applied to fracture that is accompanied by relatively little deformation or material flow in the crack area. Impact-type and fatigue-type loadings often result in brittle failure. Preventing this type of fracture through proper design is a prime concern for manufacturers and users of plastic materials, especially for glassy polymers such as polystyrene and polymethyl methacrylate.

However, a different type of brittle behaviour has been reported in polyethylene (PE); it is associated with long-term low-level loading conditions, and is referred to as "stress cracking". In contrast to instantaneous impact-type fracture, failures of this type usually develop over a relatively long period and are characterized by a slow crack growth. This crack growth can be either intrinsic or environmentally assisted.

Although both stress cracking and impact-type failure are termed brittle (in both cases due to the lack of any visible ductility on the fracture surface), the failure modes are fundamentally different. Impact failures often display crack-growth rates close to the speed of sound; stress cracking is characterized by a crack that propagates over a period ranging from a few minutes to many years.

Another important difference between impact failure and stress cracking in PE is the temperature response of the material. While impact failure in PE tends to occur at lower temperatures and at high loads, stress cracking displays the opposite effect. The tendency for stress cracking to occur increases with increasing temperature and occurs at loads significantly below the yield point.

Although fracture surfaces in both cases are visually smooth, they display entirely different features when examined microscopically. Impact fracture surfaces in PE have a flaky, scaly appearance (Fig. 1); this has been attributed to damage caused as microscopic cracks branch from the main fracture during impact [1]. In contrast, stress cracking displays a fibrous texture (Fig. 2).

The fibrous nature of the fracture surface strongly suggests the previous existence of a craze ahead of the crack. The appearance of a dark region at the crack tip during the growth of environmental stress cracks [2] has been interpreted as evidence of crazing. Transmission electron microscopy observations of the crack tip show a void structure, taken as further evidence of crazing [3], although no material was found to fill these voids. Earlier work has shown evidence of crazing in the environmental stress cracking in both low- and high-density polyethylene [4, 5] and recently crazing has been demonstrated in the intrinsic cracking of polyethylene in the absence of environmental stress cracking agents [6]. However, despite this evidence, an unambiguous micrographic view of the craze zone in polyethylene has yet to emerge.

In the case of polyethylene piping used in natural gas distribution, the implication of this brittle-type failure is a major concern. As a result, the work described here was carried out directly on extruded medium-density polyethylene pipe to examine the practical aspects of this phenomenon.

2. Experimental details

Medium-density pipe of 1 in. diameter was tested in a constant-tensile-load (CTL) fixture (Fig. 3). A 0.5 in. wide ring was cut from the pipe and axially notched to a length of 0.76 mm with a razor blade on both the inside and outside, to a depth of 1.5 mm at the region of minimum wall thickness and angled at 180 deg to this point. The ring specimen was then placed in the fixture and subjected to a constant load in both the

* *Present address*: AT&T Bell Laboratories, Murray Hill, New Jersey 07974–2070, USA.

0022–2461/87 $03.00 + .12

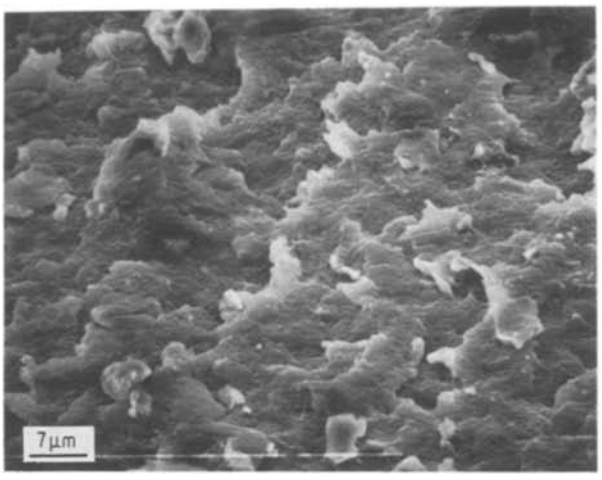

Figure 1 Scanning electron micrograph of fracture surface of medium-density polyethylene after brittle impact failure.

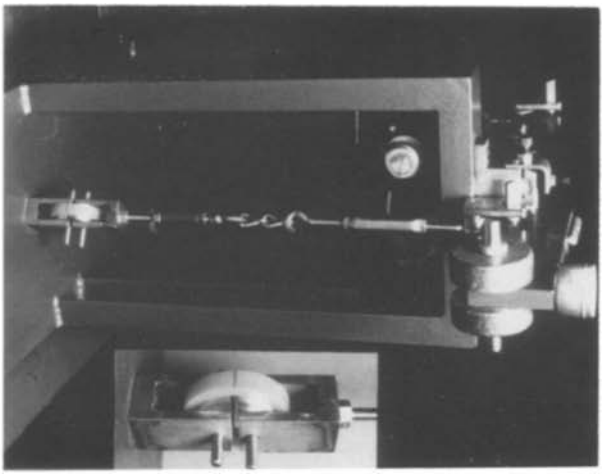

Figure 3 Constant tensile load fixture and specimen.

presence and absence of a 1% Igepal (GAF Corp.) solution at 23° C and times to failure were recorded.

Ring specimens were removed at intervals prior to complete rupture and split in two by sawing in the circumferential direction, in essence providing two rings. The crack-tip region was cut from the newly created edge of one of the rings to observe the crack in a plane strain condition. It was microtomed subsequently and etched using a permanganic acid technique [7]. The specimen was then placed under a slight three-point bend using a special fixture, coated with gold–platinum, and subsequently observed under the scanning electron microscope (SEM) while under stress. In some cases, the other ring was placed in liquid nitrogen and fractured for fracture surface observations.

The test was made on two PE samples meeting PE2306 Plastics Pipe Institute Standards designations [8]. Comonomer, molecular weight, and density data for the materials tested, labelled A-1 and B-1 are shown in Table I.

3. Results

3.1. Data

Constant tensile load data generated in air and Igepal are shown in Figs 4 and 5, respectively. The curve that is generated typically displays a shallow sloped region followed by a more steeply sloped region. Generally, ductile-type failure showing large deformation and necking, corresponding to relatively high stress levels and short failure times, occurs in the shallow-sloped region of the curve. In the region of lower stress levels and longer failure times, a brittle-type failure occurs, characterized by little deformation at the point of failure and corresponding to the region of the curve where the slope is steeper (Fig. 6). The point where the slope changes can be characterized as a type of "ductile–brittle transition", although prior use of this term generally has been limited to impact failure.

For both materials A-1 and B-1, the ductile–brittle transition occurs at approximately 70 h in Igepal (Fig. 4) while the same materials in air have a transition at approximately 160 h (Fig. 5). It should be noted that although the transitions in this case coincide for the two materials, these transitions vary significantly for other polyethylene piping materials which were tested [9].

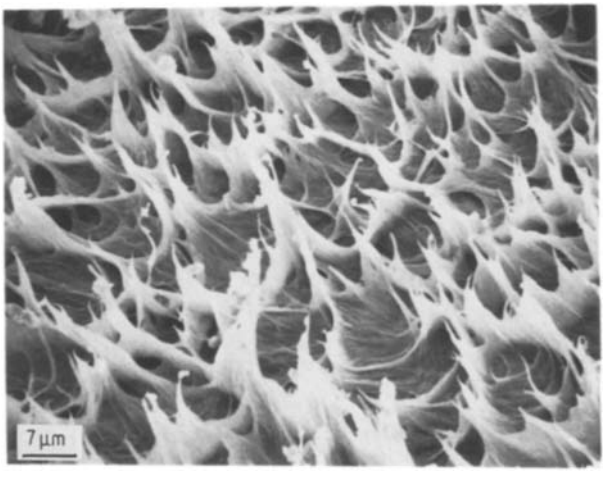

Figure 2 Scanning electron micrograph of fracture surface of medium-density polyethylene after stress cracking.

3.2. Microscopic observations

Both A-1 and B-1 samples tested at 8.3 MPa were removed from the test at various intervals prior to failure as described above. As can be seen in Figs 4 and 5, at this stress level, failures would have taken place at approximately 70 and 1000 h in Igepal and air, respectively.

The crack tip is shown under low magnification in Fig. 7 as it appears upon removal from the test after 10, 30, and 50 h. A primary craze zone is evident directly ahead of the tip of the razor notch which extends 0.38, 0.65, and 1.0 mm, respectively. In

TABLE I Characterization of resins used in tested PE pipes

Sample	Comonomer in resin	Molecular weight (10^4)			
		M_n	M_w	M_z	Density ($g\,cm^{-3}$)
A-1	Butene	2.43	10.65	61.0	0.9406
B-1	Hexene	1.44	11.55	80.7	0.9406

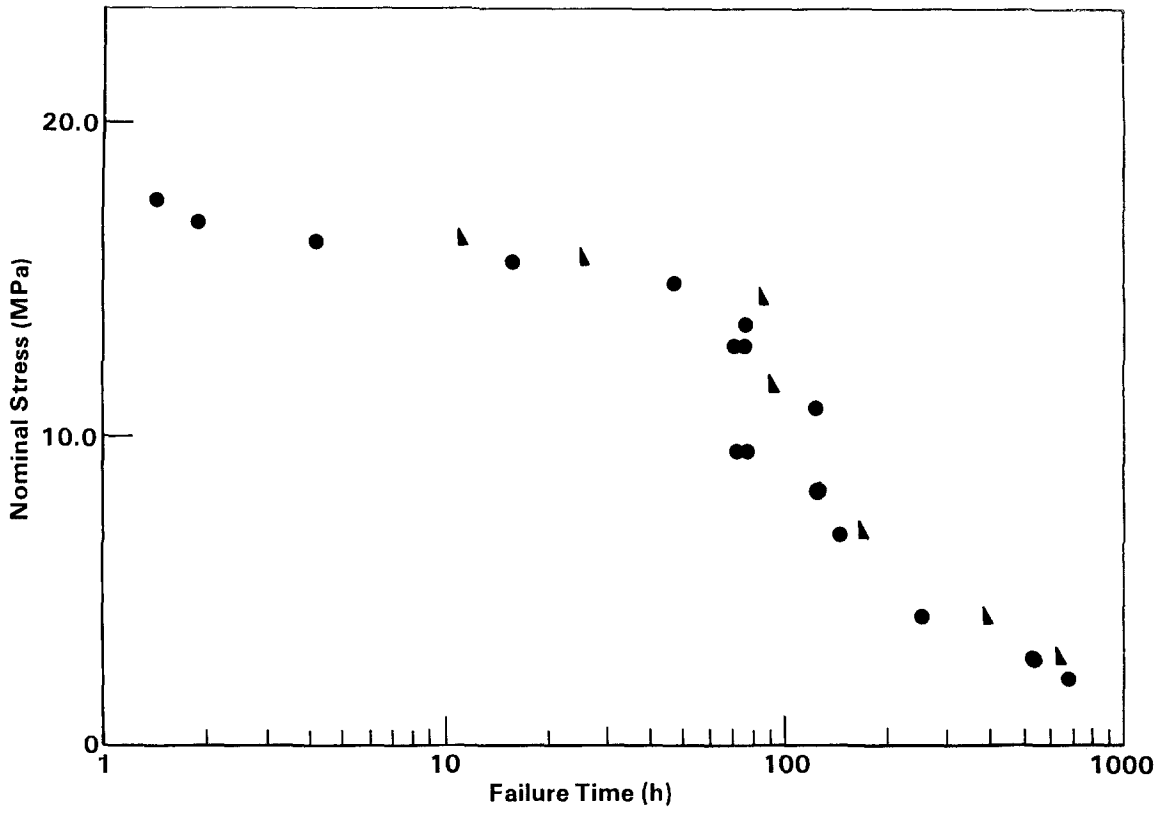

Figure 4 Constant tensile load data for two polyethylene materials in Igepal. (●) A-1, (▲) B-1.

addition, two secondary craze zones emanate at angles from the tip of the razor notch. The craze zone at the tip of the notch widens with time from 0.030 mm (10 h) to 0.063 mm (30 h) to 0.1 mm (50 h), suggesting an approximate 10 : 1 craze-length : craze-width ratio (at notch tip). The increasing craze width is due to the formation and growth of smaller parallel crazes, which ultimately connect with the primary craze (Fig. 8).

After 60 h, the craze breaks down catastrophically into a crack; a second craze subsequently forms (Fig. 9). The matching half of the sample was fractured in liquid nitrogen. As expected, this sample shows two discrete regions (Fig. 10), separated by a

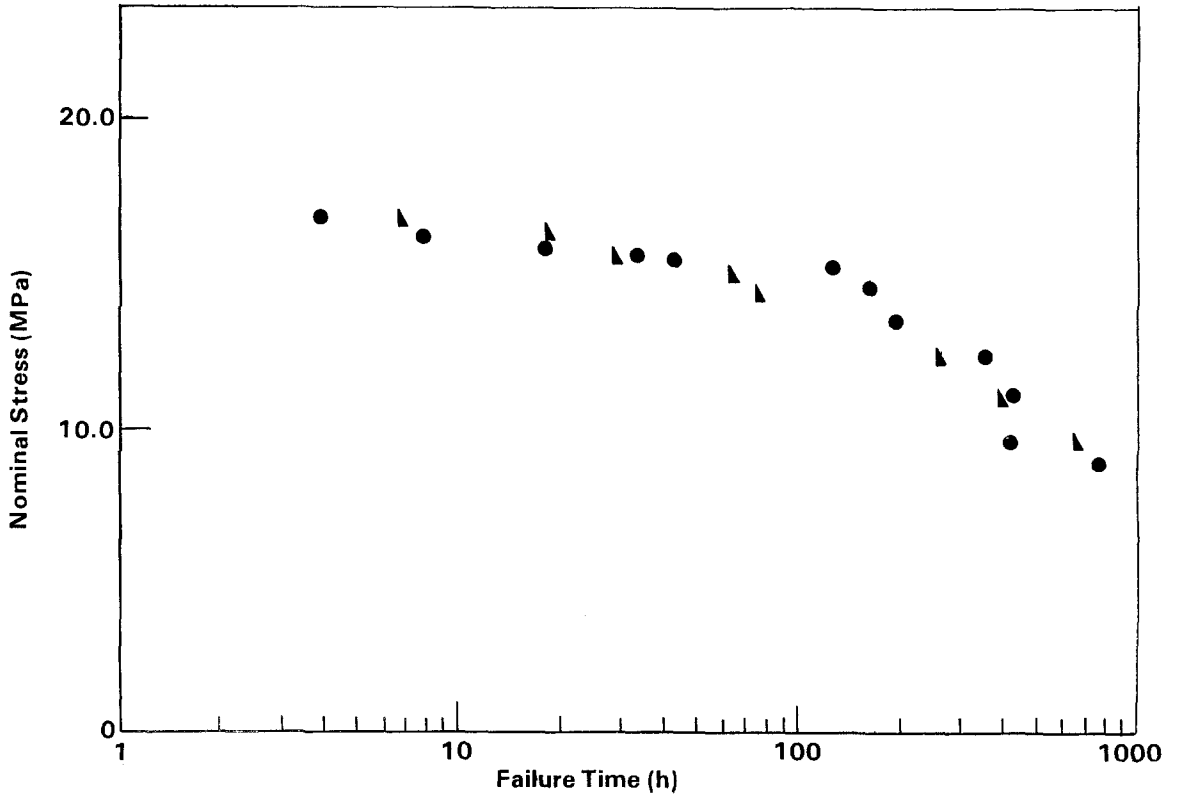

Figure 5 Constant tensile load data for two polyethylene materials in air. (●) A-1, (▲) B-1.

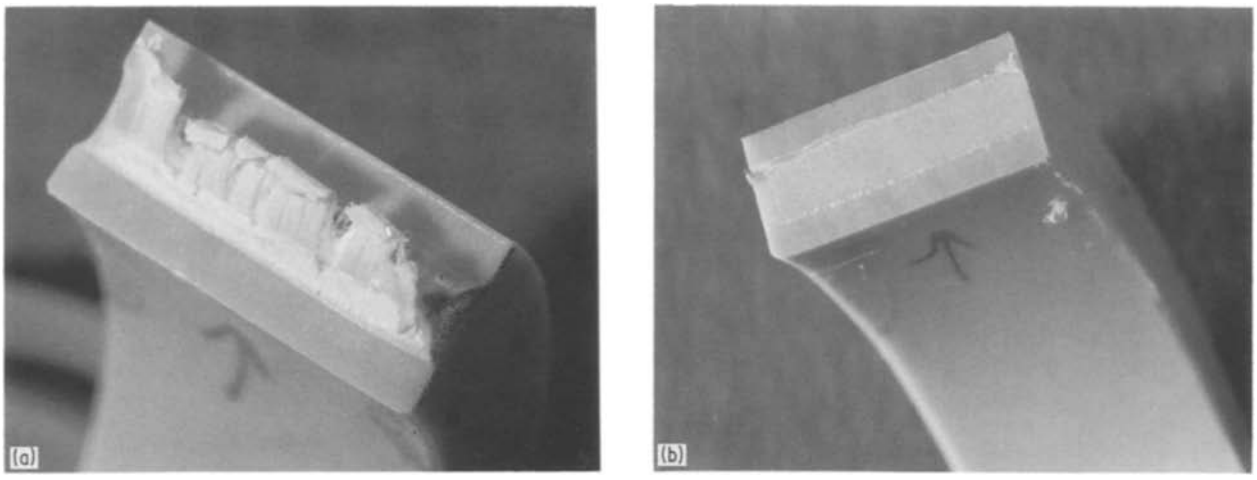

Figure 6 Fracture surfaces of constant tensile load specimens: (a) ductile failure from shallow sloped region of the curve, (b) brittle failure from steeply sloped region of the curve.

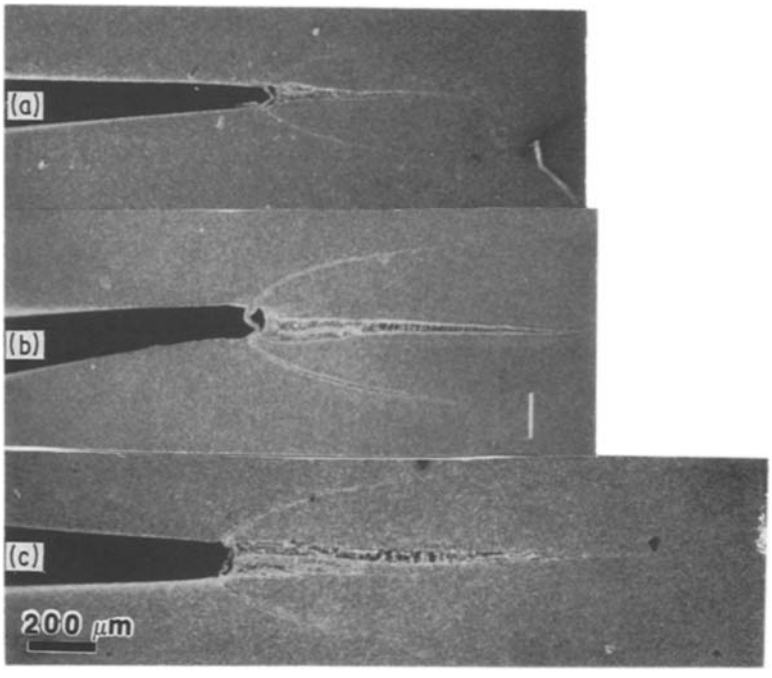

Figure 7 Primary and secondary craze growth at the tip of the razor notch in A-1 material: (a) After 10 h, (b) after 30 h, and (c) after 50 h in the constant tensile load test in Igepal.

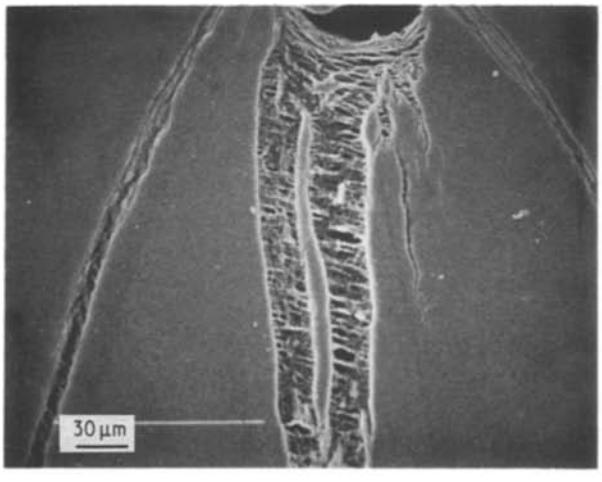

Figure 8 Higher magnification views of craze region near crack tip in 30 h specimen showing formation of small crazes parallel to primary craze.

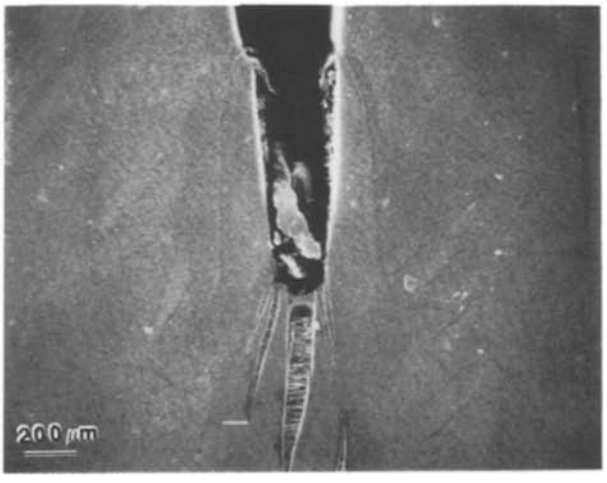

Figure 9 Primary and secondary craze growth at the tip of the crack formed by the prior breakdown of craze material after 60 h on test.

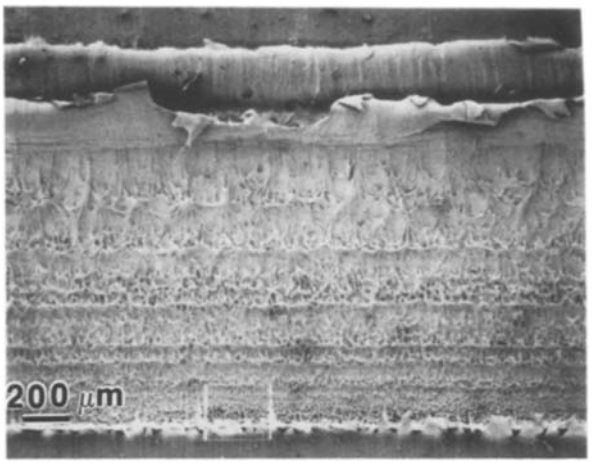

Figure 10 Fracture surface of specimen after 60 h on test after fracture in liquid nitrogen.

region of ductility corresponding to the line of crack arrest.

When this same material was removed from a CTL test (8.3 MPa) in air after 200 h, a similar craze zone was evident, but without evidence of secondary crazing (Fig. 11).

Sample B-1, when subjected to the CTL test in Igepal at 8.3 MPa, exhibited primary and secondary craze features similar to sample A-1. Fig. 12 shows a sequence of photographs similar to Fig. 7, but taken much earlier in the craze formation. They show a primary craze that had extended for 0.13 mm within the first hour after loading. Because this material fails in 70 h at this stress level, it appeared that within the first 1.5% of the material's life, the PE showed evidence of craze damage in 18% of the ligament.

Later in time after initial craze breakdown, many secondary crazes were evident (Fig. 13). The fracture surface of the matching half that was fractured in liquid nitrogen is also shown juxtaposed on the figure. The onset of secondary craze formation after initial craze breakdown corresponded exactly with what appeared to be arrest lines on the fracture surface. Therefore, it appears that in contrast to sample A-1, which experienced only one start–stop event, sample B-1 experienced at least four such events.

As in the case of A-1 material, which failed in air after 8.3 MPa in the CTL test, the B-1 material showed no evidence of secondary crazing after testing in air at 8.3 MPa and 200 h (Fig. 14). However, discrete intervals of protruding fibres on the wall of the crack again suggest that a stick–slip mechanism was operative in the B-1 material. The fracture surface of this material after total failure in the CTL test is shown in Fig. 15, again demonstrating numerous arrest lines.

4. Discussion

Interlamellar failure is the proposed rationale for environmental stress cracking [10, 11]. More specifically, evidence has been presented that tie molecules connecting lamellae are plasticized in the presence of Igepal [12–14]. However, in the light of constant tensile load data, interlamellar failure is an intrinsic phenomenon, an effect that is merely accelerated by the presence of Igepal.

Brittle failure can thus be viewed as a rate-dependent process, i.e. given enough time at stresses below those resulting in ductile failure, tie molecule entanglements will relax, resulting in brittle failure without any environment to "lubricate" the tie molecules, although the failure will be accelerated in the presence of such a "lubricant" or plasticizer.

As is clear from the microscopic craze observations, discrete fibres do, in fact, appear during craze deformation. However, as the fibres are discrete and relatively short, this suggests that considerable interference to uniform fibre deformation has occurred, because of interlamellar failure between the existing fibres. If fibre deformation was uninterrupted, the fibres would become very long in the crack-tip area, resulting in the large deformation evident in Fig. 6a.

An observable microscopic difference between intrinsic cracking and environmental stress cracking is the formation of secondary crazes in the latter. These secondary crazes do not seem to play any role in crack growth. It is possible that this formation is due to a circular yielded process zone at the notch tip upon initial deformation, and as a result, in addition to the primary craze, secondary crazes form at the stressed regions at the boundary of the process zone. In the

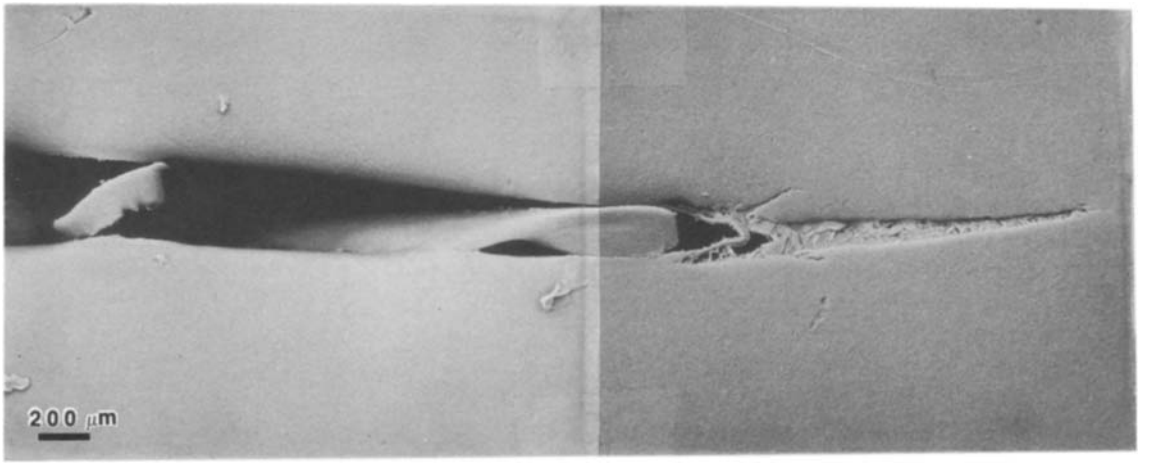

Figure 11 Craze growth and breakdown in A-1 after 200 h in the constant tensile load test in air.

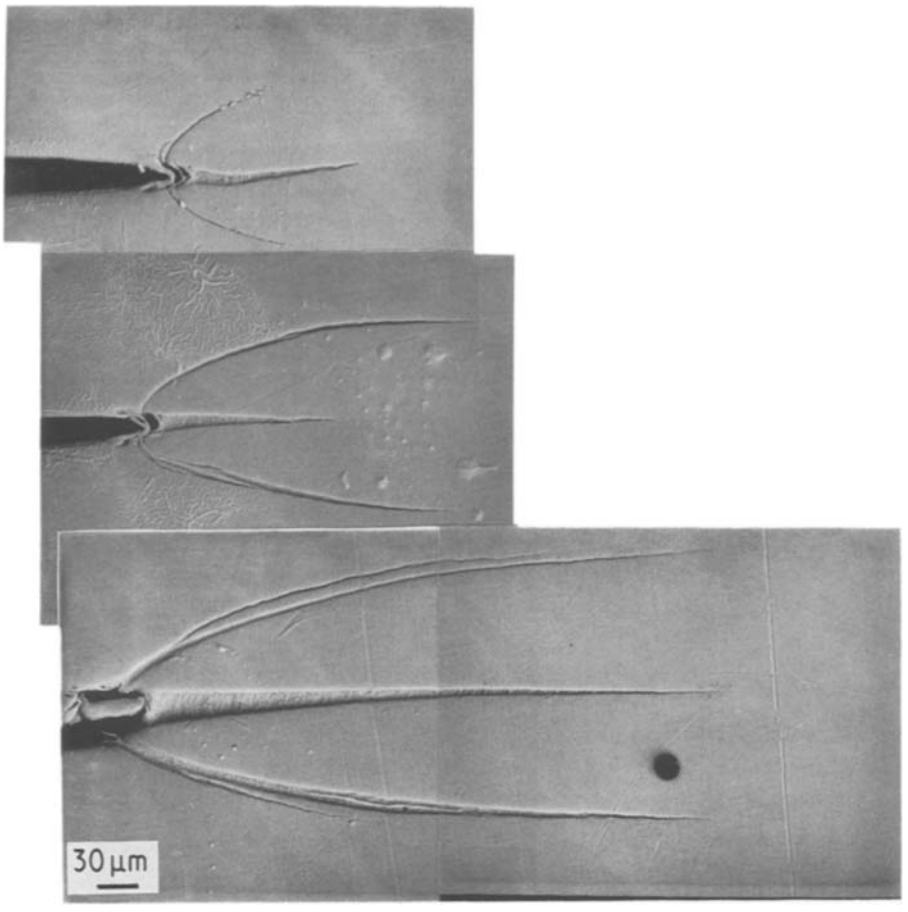

Figure 12 Craze growth at the notch tip in B-1 after: (a) 1 h, (b) 5 h, (c) 10 h on the constant tensile load test in Igepal.

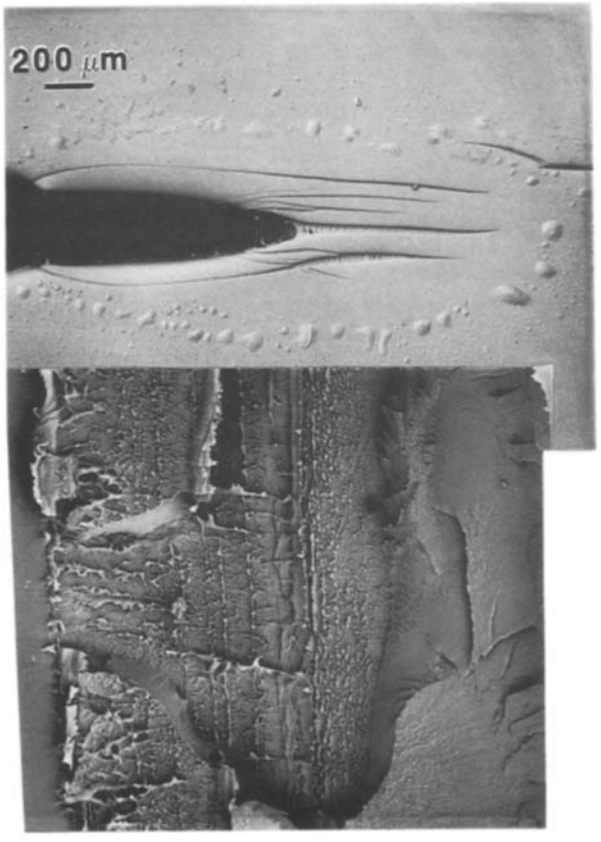

Figure 13 Craze growth and breakdown in B-1 just prior to failure in the constant tensile load test in Igepal (fracture surface is juxtaposed at same magnification illustrating arrest line).

absence of Igepal, the material is not as susceptible to craze initiation at the boundary of the process zone which is a region of lower stress and as a result secondary crazes do not form during testing in air.

It should also be noted that the fibre density in the craze is much higher after testing in air as opposed to testing in Igepal. This again is attributable to the greater tendency towards interlamellar failure in the presence of the stress-cracking environment.

The observed phenomenon of crack arrest under load is more evident in the B-1 material than in A-1. It is unclear if this difference can be attributed to the comonomer or molecular weight variations between the two resins as shown in Table I. The ability to arrest the growing crack is apparently unrelated to the failure time in the CTL test, because, as shown in Figs 4 and 5, the failure curves are virtually identical for the two materials.

A similar crack arrest and growth mechanism was inferred for polymethyl methacrylate under static loading based on similar fracture surface features resembling arrest lines [15, 16], although the phenomenon as yet had not been documented for polyethylene.

5. Conclusions

The primary mechanism of "brittle" stress cracking in medium-density polyethylene, in both the presence or absence of the Igepal environment, is craze growth and breakdown. The appearance of such a craze zone

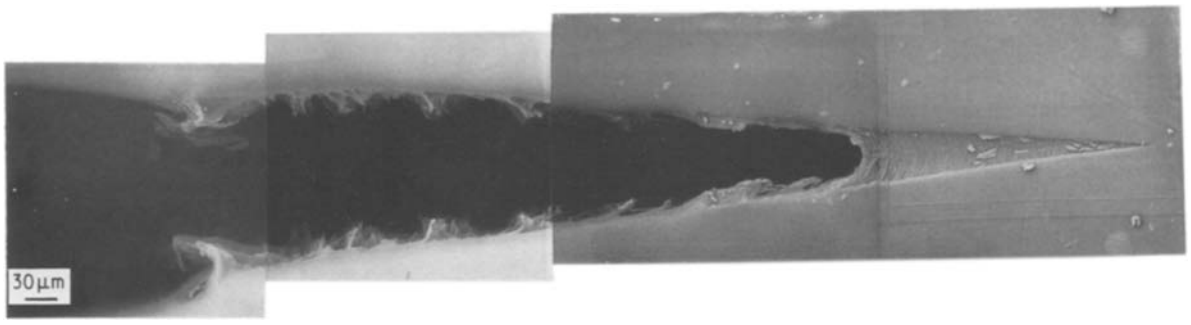

Figure 14 Craze growth and breakdown in B-1 after 200 h in the constant tensile load test in air.

suggests interlamellar failure as the molecular process for cracking under static loading conditions, because the uniform fibre deformation and the resulting high elongations at the crack tip associated with ductile failure are absent. Secondary crazes and a very low fibre density are evident in samples which failed in Igepal, due to the tendency of the environment to accelerate brittle failure at lower stresses.

Acknowledgement

The authors would like to thank the Gas Research Institute for sponsoring this research under Contract 5014-352-0613.

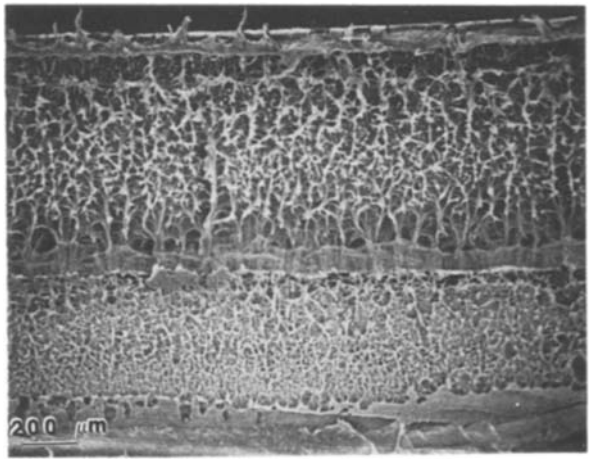

Figure 15 Fracture surface of B-1 after failure in the constant tensile load test in air.

References

1. C. G. BRAGAW, *Polym. Plast. Tech. Appl.* **1** (1979) 145.
2. S. BANDOPADHYAY and H. R. BROWN, *Polym. Eng. Sci.* **20** (1980) 720.
3. R. A. BUBECK and H. M. BAKER, *Polymer* **23** (1982) 1680.
4. A. LUSTIGER and R. D. CORNELIUSSEN, *J. Polym. Sci. B* **17** (1979) 269.
5. *Idem, Mater. Sci. Eng.* **33** (1978) 117.
6. X. LU and N. BROWN, *J. Mater. Sci.* **21** (1986) 2423.
7. R. H. OLLEY and D. C. BASSETT, *Polymer* **23** (1982) 1707.
8. ASTM Standard D3350-78.
9. A. LUSTIGER and R. L. MARKHAM, *Polymer* **24** (1983) 1647.
10. S. BANDOPADHYAY and H. R. BROWN, *ibid.* **19** (1978) 589.
11. C. J. SINGLETON, E. ROCHE and P. GEIL, *J. Appl. Polym. Sci.* **21** (1977) 2319.
12. P. D. FRAYER, P. P. L. TONG and W. W. DREHER, *Polym. Eng. Sci.* **17** (1977) 27.
13. H. R. BROWN, *Polymer* **19** (1978) 1186.
14. A. LUSTIGER and R. D. CORNELIUSSEN, *J. Polym. Sci. B* **24** (1986) 1625.
15. R. P. KUSY and D. T. TURNER, *Polymer* **18** (1977) 390.
16. R. P. KUSY, *J. Mater. Sci.* **11** (1976) 1381.

Received 19 August
and accepted 25 September 1986